Trapping energy of a spherical particle on a curved liquid interface

Joseph Léandri, Alois Würger

Trapping energy of a spherical particle on a curved liquid interface

Joseph Léandri and Alois Würger
LOMA, Université de Bordeaux & CNRS, 351 cours de la Libération, 33405 Talence, France

We derive the trapping energy of a colloidal particle at a liquid interface with contact angle θ and principal curvatures c_1 and c_2. The boundary conditions at the particle surface are significantly simplified by introducing the shift ε of its vertical position. We discuss the undulating contact line and the curvature-induced lateral forces for a single particle and a pair of nearby particles. The single-particle trapping energy is found to increase with the square of the mean curvature $c_1 + c_2$ and to decrease with the square of the anisotropy $c_1 - c_2$. Thus particles on a minimal surface ($c_1 + c_2 = 0$) move toward strongly curved regions, whereas on a deformed droplet they migrate to flatter areas.

PACS numbers:

I. INTRODUCTION

Colloidal particles trapped at a liquid phase boundary are subject to capillary forces which induce pattern formation and directed motion [1–3], and contribute to stabilize Pickering emulsions and particle aggregates [4, 5]. Such microstructures affect the mechanical and flow behavior of liquid and gel phases [6], which in turn are relevant for material properties and biotechnological applications [7]. In many instances, the particles are trapped at curved liquid interfaces; rather surprisingly, even for spherical particles the influence of curvature on capillary forces is not fully understood at present.

At a flat interface, capillary phenomena arise from normal forces induced by the particle's weight or charge, or from geometrical constraints due to its shape [8, 9]. As a simple example, an oat grain floating on a cup of milk is surrounded by a meniscus that results from the its weight and buoyancy; the superposition of the dimples of nearby grains reduces the surface energy and thus causes aggregation. Charged beads exert electric stress on the interface. The meniscus overlap of nearby particles causes a repulsive electrocapillary potential [10, 11], whereas beyond the superposition approximation, a significantly larger attractive term is found [12, 13]. In the absence of gravity and electric forces, capillary phenomena still occur for non-spherical particles: A capillary quadrupole may arise from surface irregularities [14], pinning of the contact line [15], and for ellipsoids [16–19], and favors the formation of clusters with strong orientational order.

A more complex situation occurs for interfaces with principal curvatures c_1 and c_2. The superposition of the weight-induced meniscus and the intrinsic curvature results in a coupling energy that is linear in the mean curvature $H = c_1 + c_2$. Its spatial variation gives rise to a lateral force that drags a colloidal sphere along the curvature gradient [20, 21]. Non-spherical particles interact through their capillary quadrupole with the curvature difference $\delta c = c_1 - c_2$, and thus experience both a torque and lateral force [22]. The latter is well known from the locomotion of meniscus-climbing insects and larvae, which bend their body according to the local curvature such that the capillary energy overcomes gravity [23, 24]; through a similar effect, ellipsoidal particles prevent ring formation of drying coffee stains [25, 26]. A recent experiment on micro-rods trapped at a water-oil meniscus illustrates both rotational and translational motion driven by curvature [3].

FIG. 1: Three-phase boundary of a spherical particle at a liquid interface with curvatures $c_2 = -\frac{1}{2}c_1$. The contact line is not a circle but undulates in space.

In this paper, we evaluate the geometrical part of the trapping energy of a spherical particle on a curved interface; thus we consider only terms that arise from the interface profile but are independent of body forces such as weight and buoyancy. Previous papers considered limiting cases such as a minimal surface ($H = 0$) [27], a spherical droplet ($\delta c = 0$) [28, 29], or a cylindrical interface ($H = \delta c$) [30]; yet a comprehensive picture is missing so far. Here we treat the general case where both H and δc are finite, and obtain the trapping energy in a controlled approximation to quadratic order in the curvature parameters.

As an original feature of the formal apparatus, we introduce the curvature-induced shift ε of the vertical particle position as an adjustable parameter, in addition to the amplitude ξ_2 of the quadrupolar interface deformation. As a main advantage, the boundary conditions at the contact line separate in two independent equations for ε and ξ_2, which are readily solved and provide a simple physical picture for the effects of the two curvature parameters.

The paper is organized as follows. Section 2 gives a detailed derivation of the trapping energy as a function of the parameters H and δc, and the unknowns ε and ξ_2. In Section 3, we impose Young's law at the three-phase boundary, and determine ε and ξ_2 as a function of curvature. In Section 4 we compare the trapping energy with previous work, and discuss the contact line and curvature-induced forces. Section 5 contains a brief summary.

II. TRAPPING ENERGY

Here we derive the expression for the trapping energy and then evaluate it explicitly to quadratic order in the curvatures. First consider a particle dispersed in the liquid phase with the smaller surface tension $\gamma_m = \min(\gamma_1, \gamma_2)$. The total energy $\gamma S_0 + \gamma_m 4\pi a^2$ accounts for the interface area S_0 and for the particle surface $4\pi a^2$, as illustrated in Fig. 2a.

A particle approaching the interface gets trapped if the surface tensions satisfy the inequality $|\gamma_1 - \gamma_2| < \gamma$. Imposing local mechanical equilibrium relates these parameters to the contact angle θ at the three-phase line in terms of Young's law

$$\gamma_1 - \gamma_2 = \gamma \cos\theta. \tag{1}$$

The situation shown in Fig. 2 corresponds to $\gamma_m = \gamma_2$, that is, a contact angle $\theta < \frac{\pi}{2}$. The total energy consists of the particle segments in contact with the two phases, $\gamma_1 S_1 + \gamma_2 S_2$, plus a term γS proportional to the area of the liquid interface.

The trapping potential is given by the energy difference of these two situations,

$$E = \gamma_1 S_1 + \gamma_2 S_2 + \gamma S - \gamma S_0 - \gamma_m 4\pi a^2. \tag{2}$$

As illustrated in Fig. 2b, S is smaller than the unperturbed area S_0. Since Young's law needs to be satisfied everywhere along the three-phase contact line, S may show a significantly more complex profile than S_0.

A. Flat interface $H = 0 = \delta c$

We briefly recall the well-known results for zero curvature $w_0 = 0$, where both S_0 and S are flat [1]. Then the area of the liquid interface is reduced by

$$S - S_0 = -\pi r_0^2,$$

and the segments of the particle surface read

$$S_1 = 2\pi a^2 - 2\pi a z_0, \qquad S_2 = 2\pi a^2 + 2\pi a z_0.$$

Here and in the following we use the vertical and radial coordinates of the contact line,

$$z_0 = a\cos\theta, \qquad r_0 = a\sin\theta,$$

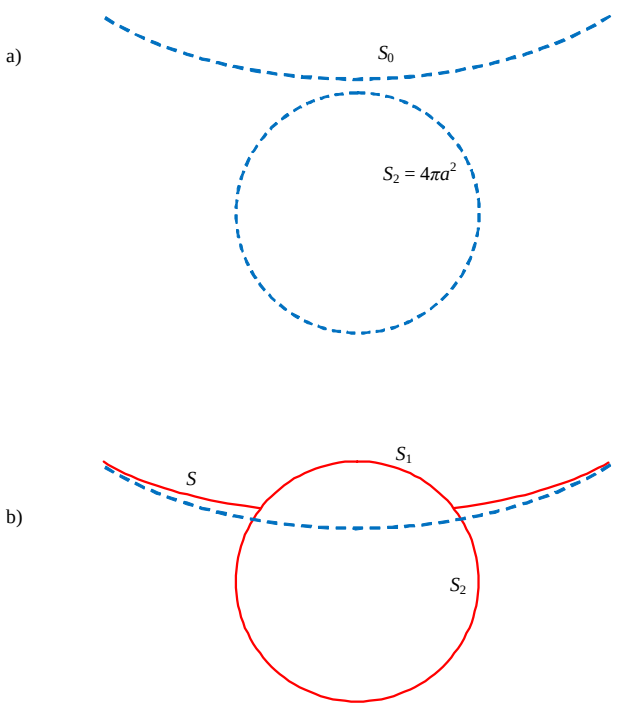

FIG. 2: Surface and interface areas contributing to the trapping energy in Eq. (2). The upper liquid is labelled "1" and the lower "2". a) The particle is in the phase of lower surface energy (here $\gamma_2 < \gamma_1$); the liquid interface of area S_0 is described by (4). b) Trapped state. The presence of the particle reduces the area of the liquid phase boundary to the value S and deforms its profile. The surface areas S_1 and S_2 are in contact with the two liquid phases. Note that the figure shows one vertical section of the interface; both S_0 and S undulate when rotating about the vertical axis.

as illustrated in the left panel of Fig. 3. With Young's law one finds for a flat interface [1],

$$E_0 = -\pi a^2 \gamma (1 - |\cos\theta|)^2. \tag{3}$$

The trapping energy vanishes for contact angles $\theta = 0$ and $\theta = \pi$. For $|\gamma_1 - \gamma_2| > \gamma$ Young's law has no solution, meaning that there is no stable trapped state.

B. Finite curvature

The profile of a curved interface in Monge representation reads as $w_0 = \frac{1}{2}\left(c_1 u^2 + c_2 v^2\right)$, with the coordinates u and v along the local principal curvature axes. For later convenience we transform to polar coordinates; inserting $u = r\cos\varphi$ and $v = r\sin\varphi$, resulting in

$$w_0(r,\varphi) = \frac{r^2}{4}\left(H + \delta c\ \cos(2\varphi)\right). \tag{4}$$

The axes are chosen such that both H and δc are positive.

The unperturbed interface profile w_0 is related to the pressure difference P and the tension γ, according to the Young-Laplace equation

$$\boldsymbol{\nabla}^2 w_0 + P/\gamma = 0, \tag{5}$$

where $\boldsymbol{\nabla}$ is the 2D gradient in the $u-v$-plane. Experimentally a curved interface is realized by applying body forces, hydrostatic pressure, or appropriate boundary conditions.

The quadratic form (4) provides a good approximation at distances within the curvature radius

$$R = 2/\sqrt{H^2+\delta c^2}.$$

In the case of a spatially varying curvature, the parameters H and δc change in general on the scale of the curvature radius. Like previous papers, the present work relies on the separation of length scales, assuming that the characteristic length of the deformation induced by a colloidal particle of size a, is much larger than that of the unperturbed interface, R. All approximate formulae of the present paper can be cast in the form of a truncated series in powers of $1/R$, and the trapping energy derived below is exact to quadratic order.

C. Interface area

Now we add a colloidal particle to the interface (4). Because of the undulating contact line, Young's law cannot be satisfied along the intersection of $w_0(r,\varphi)$ and the spherical bead, but requires a modified interface profile

$$w = w_0 + \xi. \tag{6}$$

The deformation field ξ is chosen such that the contact angle θ is realized everywhere along the three-phase boundary.

The deformation field ξ affects the trapping energy in two respects: First, it results in a more complex profile of the liquid interface S, and, second, it modifies the contact line, that is, the common boundary of S, S_1, and S_2. We start with the liquid-interface areas S and S_0; their formally exact expressions depend on $\boldsymbol{\nabla} w$ and $\boldsymbol{\nabla} w_0$, respectively [27]. The unperturbed interface profile (4) relies on the small-gradient approximation $|\boldsymbol{\nabla} w_0| \ll 1$ in the vicinity of the particle. Accordingly, we truncate at quadratic order in $\boldsymbol{\nabla} w$ and $\boldsymbol{\nabla} w_0$, and find for the change of interface area

$$\begin{aligned} S - S_0 &= \frac{1}{2}\int_{\mathcal{I}} dA \left((\boldsymbol{\nabla} w)^2 - (\boldsymbol{\nabla} w_0)^2 \right) - \int_{\mathcal{I}} dA \frac{P}{\gamma}\xi \\ &\quad - \int_{\mathcal{P}} dA \left(1 + \frac{1}{2}(\boldsymbol{\nabla} w_0)^2 \right). \end{aligned} \tag{7}$$

The first integral accounts for the change of area of the deformed interface, the second one for the work done by the Laplace pressure P, and the third one for the area occupied by the particle. Projection on the tangential plane defines the parameter domains $\mathcal{I}$ and $\mathcal{P}$, and their boundary $\partial\mathcal{P}$ corresponds to the projection of the contact line.

The first integral in (7), over the domain $\mathcal{I}$, is evaluated according to the usual procedure [27]: Integrating by parts and inserting $w = w_0 + \xi$, we find a line integral along $\partial\mathcal{P}$ that is given below, and the surface integral of $-\frac{1}{2}\xi\boldsymbol{\nabla}^2\xi - \xi\boldsymbol{\nabla}^2 w_0$. The latter term cancels the Laplace pressure according to (5). Minimizing the former with respect to ξ, we find that the deformation satisfies the equation of a minimal surface

$$\boldsymbol{\nabla}^2 \xi = 0. \tag{8}$$

Regarding the third integral, which runs over the domain $\mathcal{P}$, we calculate

$$(\boldsymbol{\nabla} w_0)^2 = r^2 \frac{H^2 + \delta c^2 + 2\mathcal{C}_2 H \delta c}{4},$$

with the shorthand notation $\mathcal{C}_2 = \cos(2\varphi)$. Integrating the radial part of $dA = dr r d\varphi$, we find

$$\begin{aligned} S - S_0 &= -\frac{1}{2}\oint_{\partial\mathcal{P}} d\mathbf{s}\cdot(\boldsymbol{\nabla}\xi + 2\boldsymbol{\nabla} w_0)\,\xi \\ &\quad - \int_0^{2\pi} d\varphi \left(\frac{\widetilde{r}^2}{2} + \frac{\widetilde{r}^4}{32}\left(H^2 + \delta c^2 + 2\mathcal{C}_2 H\delta c\right)\right), \end{aligned}$$

where $\widetilde{r}(\varphi)$ is the radial coordinate of the contact line.

The integrand of the first term is of second order in the curvature-induced deformation field ξ. Thus we evaluate the contour at order zero, replace the gradients with the radial components $\partial_r\widetilde{\xi} + 2\partial_r\widetilde{w}_0$, and use $r_0\partial_r\widetilde{w}_0 = 2\widetilde{w}_0$. By the same token, in the last term which is quadratic in the curvatures, we replace the radius of the contact with its unperturbed expression, $\langle\widetilde{r}^4\rangle = r_0^4$. This gives

$$\begin{aligned} S - S_0 &= -\pi\langle(r_0\partial_r\widetilde{\xi} + 4\widetilde{w}_0)\widetilde{\xi}\rangle \\ &\quad -\pi\langle\widetilde{r}^2\rangle - \frac{\pi r_0^4}{16}\left(H^2+\delta c^2\right), \end{aligned} \tag{9}$$

where we have introduced the shorthand notation for the azimutal integral

$$\int_0^{2\pi} d\varphi(...) = 2\pi\,\langle ...\rangle\,.$$

The particle segments in contact with the two liquid phases are given by the vertical coordinate $\widetilde{z}(\varphi)$ of the contact line with respect to the particle center,

$$S_1 = 2\pi a^2 - 2\pi a\,\langle\widetilde{z}(\varphi)\rangle\,, \tag{10}$$

$$S_2 = 2\pi a^2 + 2\pi a\,\langle\widetilde{z}(\varphi)\rangle\,. \tag{11}$$

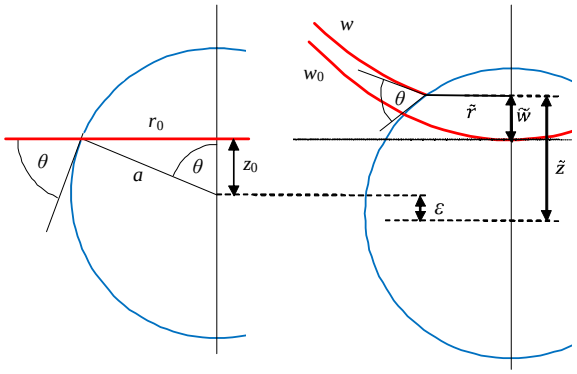

FIG. 3: Side view on a sphere trapped at a liquid phase boundary. The left panel shows a flat interface, where $r_0 = a\sin\theta$ and $z_0 = a\cos\theta$ are the radial and vertical coordinates of the contact line with respect to the particle center. The right panel illustrates the case of finite curvature. In a vertical section of given azimuth, we show both the unperturbed interface w_0 and the deformed profile w. Two phenomena concur in order to satisfy Young's law: The interface profile changes by $\xi = w - w_0$, and the particle adjusts its vertical position by ε. Besides its radial coordinate $\tilde{r}$, we indicate the vertical position of the contact line with respect to the tangent plane, $\tilde{w}$, and with respect to the particle center, $\tilde{z} = z_0 + \tilde{w} + \varepsilon$. In the case of finite curvature anisotropy δc, the contact line is not a circle but undulates along the particle surface, as illustrated by the top view in Fig. 4.

D. Curvature-induced energy

The interface and surface areas give the trapping energy (2) as a function of the coordinates $\widetilde{r}$ and $\widetilde{z}$ of the undulating contact line, which both depend on the azimuthal angle φ. The curvature-induced change of the vertical position with respect to that on a flat interface comprises two terms,

$$\widetilde{z} = z_0 + \widetilde{w} + \varepsilon, \tag{12}$$

where $\widetilde{w}$ accounts for the vertical displacement of the contact line on the particles surface, and ε for the change in the particle position with respect to the tangential plane, as illustrated in the right panel of Fig. 3.

Any point at the surface of the sphere satisfies the condition $\widetilde{r}^2 + \widetilde{z}^2 = a^2$, which can be rewritten as

$$\widetilde{r}^2 = r_0^2 - 2z_0\,(\widetilde{w} + \varepsilon) - (\widetilde{w} + \varepsilon)^2. \tag{13}$$

This relation simplifies the second term in (9).

Inserting these expressions in (2) and separating the terms on a flat interface from the contributions that depend on curvature, we find

$$\begin{aligned} E - E_0 \;=\; & -\pi\gamma\langle(r_0\partial_r\widetilde{\xi} + 4\widetilde{w}_0)\widetilde{\xi}\rangle \\ & +\pi\gamma\langle(\widetilde{w} + \varepsilon)^2\rangle - \pi\gamma\frac{r_0^4}{16}\left(H^2 + \delta c^2\right). \end{aligned} \tag{14}$$

Note that the contributions linear in $\widetilde{w} + \varepsilon$ have disappeared: The term in $S - S_0$ stemming from $\langle\widetilde{r}^2\rangle$, exactly cancels that arising from $\gamma_1 S_1 + \gamma_2 S_2$. The remainder is of quadratic order in the parameters H and δc, in the curvature-induced deformation amplitude ξ, and in vertical shift ε of the particle position.

Regarding the deformation field, the general solution of (8) reads $\xi_0 \ln r + \sum_k \xi_k\,(r_0/r)^k \cos(k\varphi)$. Because of the twofold symmetry of the source field (4), the quadrupolar term $k = 2$ is the only contribution that is linear in the curvature. Thus we write

$$\xi = \xi_2\,(r_0/r)^2 \cos(2\varphi) \tag{15}$$

and discard quadratic and higher-order terms in ξ. For notational convenience we rewrite shift and modulation of the contact line as

$$\widetilde{w}_0 = \omega_0 + \omega_2\cos(2\varphi),$$

with the parameters

$$\omega_0 = \frac{1}{4}Hr_0^2, \qquad \omega_2 = \frac{1}{4}\delta c r_0^2. \tag{16}$$

Inserting these expressions in (14) and performing the integrals over the azimuthal angle φ, we obtain

$$\begin{aligned} E - E_0 \;=\; & \pi\gamma\xi_2^2 - 2\pi\gamma\xi_2\omega_2 \\ & +\pi\gamma(\omega_0 + \varepsilon)^2 + \frac{\pi\gamma}{2}(\omega_2 + \xi_2)^2 \\ & -\pi\gamma\left(\omega_0^2 + \omega_2^2\right). \end{aligned} \tag{17}$$

Besides the curvature parameters ω_0 and ω_2, this energy depends on two unknown parameters, the deformation amplitude ξ_2 and the vertical shift ε of the particle position with respect to its value on a flat interface.

In view of their different sign, it is worthwhile to detail the origin of each contribution to the trapping energy. The first one, $\pi\gamma\xi_2^2$, gives the deformation energy of the liquid interface, and the second one, $-2\pi\gamma\xi_2\omega_2$, accounts for the coupling of the deformation amplitude ξ with the intrinsic curvature w_0. The remainder of (17) arises from the second integral of the interface area (7), the positive terms from the "1", and the negative one from $\frac{1}{2}\left(\boldsymbol{\nabla} w_0\right)^2$.

III. YOUNG'S LAW AT THE CONTACT LINE

The quantities ξ_2 and ε are determined from Young's law for the contact angle θ, which we write in the form [27]

$$\cos\theta = \mathbf{n}_I \cdot \mathbf{n}_P, \tag{18}$$

where $\mathbf{n}_I$ is the normal vectors on the interface and $\mathbf{n}_P$ the normal on the particle surface. The former is best given in Monge gauge with respect to the vertical axis,

and the latter takes a simple form because of the spherical geometry,

$$\mathbf{n}_I = \frac{\mathbf{e}_z - \boldsymbol{\nabla}\widetilde{w}}{\sqrt{1+(\boldsymbol{\nabla}\widetilde{w})^2}}, \qquad \mathbf{n}_P = \frac{\mathbf{e}_z\widetilde{z} + \mathbf{e}_r\widetilde{r}}{a}. \tag{19}$$

Inserting in (18) and linearizing in $\widetilde{w}$ and ε, we obtain the condition

$$\widetilde{w} + \varepsilon - r_0\partial_r\widetilde{w} = 0 \tag{20}$$

along the contact line. Taking the derivative and using the shorthand notation $\widetilde{w} = w(r_0)$ we find

$$-\widetilde{w}_0 + \varepsilon - 3\widetilde{\xi} = 0.$$

After inserting the explicit expressions for $\widetilde{w}_0$ and $\widetilde{\xi}$, and separating the constant part from the modulation, one readily solves for

$$\varepsilon = \omega_0 = \frac{r_0^2 H}{4}, \qquad \xi_2 = \frac{\omega_2}{3} = \frac{r_0^2\delta c}{12}. \tag{21}$$

In physical terms, the mean curvature results in a shift ε of the particle toward the convex side of the interface. (In Fig. 2 this means in downward direction.) On the other hand, the non-uniform curvature δc gives rise to the quadrupolar amplitude ξ_2, which in turn enhances the angular modulation of the interface.

IV. DISCUSSION

The main results of the present paper are given by Eqs. (17) and (21). Here we discuss their most important features and compare with the results of previous work.

A. Vertical particle position

Properly imposing Young's law along a non-circular contact line is not an easy matter. Eq. (18) relates the contact angle to the essential parameters, the slope of the interface, as expressed by the gradient $\nabla\widetilde{w}$, and the vertical position $\widetilde{z}$ of the contact line on the particle. Previous authors mostly chose to cast this in a geometrical relation for the angle α of inclination of the interface, $\tan\alpha = \nabla\widetilde{w}$, in the frame attached to the particle. We found it helpful to introduce the vertical shift ε of the particle position with respect to the tangential plane.

This approach leads to a rather simple relation of the contact angle to the interface deformation, in terms of (19) and (12). The resulting linearized differential equation (20) comprises two constraints: The term varying with the azimuthal angle determines the deformation amplitude ξ_2, whereas the constant provides the vertical shift ε. The rather simple solution (21) shows that the vertical shift is determined by the mean curvature, and the deformation amplitude by the anisotropy δc.

B. Trapping energy

Inserting the above expressions for ε and ξ_2 in the trapping energy, we find

$$E = E_0 + \pi\gamma r_0^4\left(\frac{3}{16}H^2 - \frac{1}{24}\delta c^2\right). \tag{22}$$

The curvature-induced correction $E - E_0$ is a quadratic function of the curvature parameters H and δc. The linear terms present in each of the areas $S - S_0$, S_1, and S_1, exactly cancel each other.

The numerical coefficients $\frac{3}{16}$ and $-\frac{1}{24}$ result from several positive and negative terms of comparable size in (17). Thus it is essential to carefully evaluate all quadratic contributions to (2). We find that a finite mean curvature H increases the energy and thus reduces the trapping strength, whereas a curvature anisotropy δc lowers the energy and enhances trapping.

We compare our Eq. (22) to the results of previous work. In an earlier paper [27], one of us considered the case of a minimal surface ($H = 0$) and found, in the notation adopted here, $E - E_0 = -\frac{1}{24}\pi\gamma r_0^4\delta c^2$, which agrees with the second term in (22). Kralchevsky et al. [28] and Komura et al. [29] treated the case of a particle trapped on a liquid droplet of radius R and mean curvature $H = 2/R$. Expanding their surface energy in powers of $1/R$ and truncating at second order, we obtain $E - E_0 = \frac{3}{16}\pi\gamma r_0^4 H^2$, in agreement with our Eq. (22). (We discard the volume enthalpy term $P_1V_1 + P_2V_2$ which Komura et al. add in view of the Laplace pressure $P_1 - P_2$.) More recently, Zeng et al. [30] considered the case of a particle trapped at a cylindrical interface of radius R, where $H = \delta c = 1/R$, and found the curvature-dependent binding energy $E - E_0 = \gamma r_0^4(\frac{3}{16}\pi - 0.533)/R^2$. The positive term agrees with our Eq. (22), whereas the negative one does not. This discrepancy could be due to the fact that in [30] the deformation amplitude is not derived from the boundary conditions but obtained from a more qualitative argument.

C. Contact line

It turns instructive to explicitly give the position of the contact line. Inserting $\widetilde{w}$ and ε in (12) we have

$$\widetilde{z} - z_0 = \frac{r_0^2 H}{2} + \frac{r_0^2\delta c}{3}\cos(2\varphi). \tag{23}$$

The right-hand side is independent of the sign of $\cos\theta$. Thus in the case a finite mean curvature H, the contact line always moves toward the convex side of the interface. If the anisotropy δc exceeds the mean curvature, the contact line may move in either direction on different parts of the contact line, depending on the ratio $\delta c/H$.

Regarding the change of the radial position, we expand (13) to linear order in $\widetilde{z} - z_0$ and find

$$\widetilde{r} - r_0 = -\frac{z_0}{r_0}\left(\frac{r_0^2 H}{2} + \frac{r_0^2\delta c}{3}\cos(2\varphi)\right). \tag{24}$$

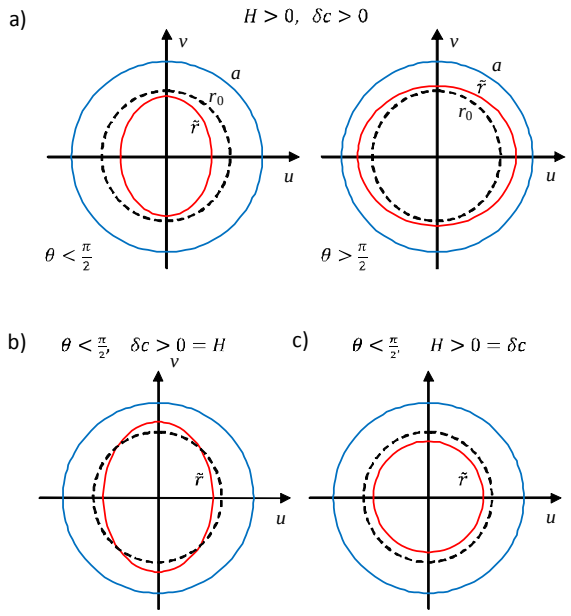

FIG. 4: Top view of the three-phase contact line on a particle of radius a. The dashed circle indicates the contact line of radius r_0 at a flat interface. The solid (red) line gives the radial coordinate $\widetilde{r}$ according to (24). a) The upper panel shows the case where both curvature parameters H and δc are positive and take similar values. For small contact angles $\theta < \frac{\pi}{2}$, the radius $\widetilde{r}$ of the contact line is reduced according to (24), whereas it increases for large contact angles $\theta > \frac{\pi}{2}$. In both cases the effect is strongest along the axis u with the largest principal curvature c_1. The lower panel illustrates the case where either H are δc vanish. b) For zero mean curvature $H = 0$, that is on a minimal surface, the radial coordinate undulates about the mean value r_0. c) In the case of zero asymmetry, $\delta c = 0$, the curvature-induced change of the radial coordinate is constant, and $\widetilde{r}$ describes a circle.

Note that r_0 is always positive, whereas $z_0 = a\cos\theta$ takes a positive sign for small contact angles $\theta < \frac{\pi}{2}$, and a negative one for $\theta > \frac{\pi}{2}$. Thus (23) and (24) have opposite sign for small contact angles, and the same sign for large θ.

The radial modulation, that is the projection of the contact line on the $u-v$-plane, is illustrated in Fig. 4. The upper panel a) shows the case of positive mean curvature H and finite δc, where the contact line moves upward and undulates around the particle; for small contact angle, the upward motion reduces the mean radius, whereas for $\theta > \frac{\pi}{2}$, it is accompanied by an increase of the radius. Fig. 4b) shows the case of zero mean curvature and finite δc, where the radius undulates along the contact line but its mean value is unchanged; a similar picture occurs for $\theta > \frac{\pi}{2}$, albeit with the axes u and v exchanged. Finally, Fig. 4c) illustrates the case $\delta c = 0$, where the contact line remains a cercle.

D. Lateral force

On an interface with spatially varying curvature, the trapping energy changes with position and thus gives rise to a lateral force $\mathbf{F} = -\boldsymbol{\nabla} E$ on the trapped particle,

$$\mathbf{F} = \pi\gamma r_0^4 \left(-\frac{3}{8} H \boldsymbol{\nabla} H + \frac{1}{12} \delta c \boldsymbol{\nabla} \delta c \right). \tag{25}$$

As shown in our previous work [27], the gradient of the curvature anisotropy pushes the particle towards more strongly curved regions of the interface. The term proportional to the gradient of the mean curvature, carries the opposite sign.

E. Two-particle interaction

Finally we discuss curvature-induced forces between neighbor particles. In a first step we derive the modified parameters $\widehat{H}$ and $\widehat{\delta c}$ that account for both the intrinsic curvature and additional terms due to a colloidal particle. The mean curvature $\widehat{H}$ is given by $\nabla^2 w = \nabla^2(w_0 + \xi)$. Since the deformation field ξ obeys the equation (8) of a minimal surface, we find $\widehat{H} = H$; in other words, the particle does not change the mean curvature of the interface.

The anisotropy is best calculated in cartesian coordinates u and v, where

$$\widehat{\delta c} = \delta c + \partial_u^2 \xi - \partial_v^2 \xi.$$

This form is readily evaluated and gives after transformation to polar coordinates

$$\widehat{\delta c} = \delta c \left(1 + \frac{r_0^4}{r^4} \cos(4\varphi) \right). \tag{26}$$

Thus the deformation field ξ significantly modifies the curvature in the vicintiy of the particle. The additonal term decays with the fourth power of the distance; because of its fourfold symmetry, the angular modulation is maximum along the principal axes u and v, and minimum in between.

Each particle feels the additional curvature induced by its neighbor. Superposition of their deformation fields gives the pair potential [27]

$$U = -\frac{\pi\gamma \delta c^2 r_0^8}{48\rho^4} \cos(4\varphi),$$

where ρ and φ describe the relative position of the particles. With the corresponding unit vectors $\mathbf{e}_\rho$ and $\mathbf{e}_\varphi$ the mutual force reads as

$$\mathbf{F}_2 = -\frac{\pi\gamma r_0^8 \delta c^2}{12\rho^5} \left(\cos(4\varphi)\mathbf{e}_\rho + \sin(4\varphi)\mathbf{e}_\varphi \right), \tag{27}$$

Thus the capillary force between two nearby particle is not a central force: Besides the attractive radial component, there is an additional force that tends to align

the particles parallel to one of the principal axes. As noted previously, the latter force favors aggregates of cubic symmetry [27].

A simple estimate shows that either of the forces F_2 and F may dominate. The curvature parameters vary on the scale of the curvature radius R, resulting in curvature-induced force $F \sim \gamma r_0^4 R^{-3}$, whereas that due to pair interactions decays on the scale of the particle distance, $F_2 \sim \gamma r_0^8 \rho^{-5} R^{-2}$. With typical values $r_0 \sim 1$ μm and $R \sim 1$ mm, one finds that the ratio $F_2/F \sim R r_0^4 \rho^{-5}$ is larger than unity at distances of a few r_0, and smaller than unity beyond.

V. SUMMARY

Starting from the well-known form (2), we have evaluated the trapping energy of a spherical particle to quadratic order in the curvature parameters.

(i) On a formal level, the introduction of the shift ε of the vertical partical position, leads to a remarkably simple equation (20) for Young's law at the three-phase boundary, which is solved in (21). This could be useful for disentangling the involved boundary condtions occurring at the surface of cylinders and ellipsoids [31], or on Janus particles [32].

(ii) As a main result, Eq. (22) shows that the mean curvature H augments the energy and thus weakens trapping, whereas the anisotropy δc lowers the energy and enhances trapping. As a consequence, on a minimal surface ($H = 0$) the curvature-induced lateral force (25) drives particles toward strongly curved regions. On the other hand, on a deformed droplet the term proportional to ∇H prevails in most cases, such that a trapped particle moves toward flatter parts of the interface.

(iii) Eqs. (23) and (24) give the radial and vertical coordinates of the undulating contact line in terms of contact angle and curvature parameters; the main dependencies are illustrated in Fig. 4.

(iv) The particle-induced interface deformation ξ is proportional to the curvature anisotropy δc but independent of the mean curvature. As a consequence, only the anisotropy gives rise to a capillary interactions of nearby particles, and the interaction potential U reduces to the form derived previously for $\delta c \neq 0 = H$.

[1] P. Pieranski, Phys. Rev. Lett., **45**, 569 (1980).
[2] N. Bowden, A. Terfort, J. Carbeck, G.M. Whitesides, Science **11**, 233 (1997)
[3] M. Cavallaro, L. Botto, E.P. Lewandowski, M. Wang, K.J. Stebe, PNAS **108**, 20923 (2011)
[4] E. Koos, N. Willenbacher, Science **311**, 897 (2011)
[5] H.-J. Butt, Science **311**, 868 (2011)
[6] R. Aveyard, B.P. Binks, J. H. Clint, Adv. Colloid Interface Sci. **100–102**, 503 (2003)
[7] C. Zeng, H. Bissig, A.D. Dinsmore, Solid State Comm. **139**, 547, (2006)
[8] D.Y.C. Chan, J.D. Henry, L.R. White, J. Colloid Interf. Sci. **79**, 410 (1981)
[9] P.A. Kralchevsky, K. Nagayama, Langmuir **10**, 23 (1994)
[10] L. Foret, A. Würger, Phys. Rev. Lett. **92**, 058302 (2004)
[11] M. Oettel, A. Dominguez, S. Dietrich, Phys. Rev E **71**, 051401 (2005)
[12] A. Würger, L. Foret, J. Phys. Chem. B **109**, 16435 (2005)
[13] M. Oettel, A. Dominguez, S. Dietrich, J. Phys. Condens. Matter **17**, L337 (2005)
[14] D. Stamou, D. Duschl, D. Johannsmann, Phys. Rev. E **62,** 5263 (2000)
[15] J.-B. Fournier, P. Galatola, Phys. Rev. E **65**, 031601 (2002)
[16] E.A. van Nierop, M.A. Stejnman, S. Hilgenfeldt, Euorphys. Lett. **72**, 671 (2005)
[17] J.C. Loudet, A.M. Alsayed, J. Zhang, A. G. Yodh, Phys. Rev. Lett. **94**, 018301 (2005)
[18] B. Madivala, J. Fransaer, J. Vermant, Langmuir **25**, 2718 (2009)
[19] E.P. Lewandowski, et al., Langmuir **26**, 15142 (2010)
[20] P.A. Kralchevsky, V.N. Paunov, N.D. Denkov, K. Nagayama, J. Colloid Interf. Sci. **167**, 47 (1994)
[21] N.D. Vassileva, D. van den Ende, F. Mugele, J. Mellema, Langmuir **21**, 11190 (2005)
[22] A. Dominguez, M. Oettel, S. Dietrich, J. Chem. Phys. **128**, 114904 (2008)
[23] D.L. Hu, J.W.M. Bush, Nature **437**, 733 (2005)
[24] J.W.M. Bush, D.L. Hu, Ann. Rev. Fluid Mech. **38**, 339 (2006)
[25] P.J. Yunker, T. Still, M.A. Lohr, A.G. Yodh, Nature **476**, 308 (2011)
[26] J. Vermant, Nature **476**, 286 (2011)
[27] A. Würger, Phys. Rev. E **74**, 041402 (2006)
[28] P.A. Kralchevsky, I.B. Ivanov, K.P. Ananthapadmanabhan, A. Lips, Langmuir **21**, 50 (2005)
[29] S. Komura, Y. Hirose, Y. Nonomura, J. Chem. Phys. **124**, 241104 (2006)
[30] C. Zeng, F. Brau, B. Davidovitcha, A.D. Dinsmore, Soft Matter **8**, 8582 (2012)
[31] L. Botto, L. Yao, R.L. Leheny, K.J. Stebe, Soft Matter **8**, 4971 (2012)
[32] B.J. Park, D. Lee, ACS Nano **6**, 782 (2012)